Meteorological, Sea Ice, and Physical Oceanographic Conditions in the Labrador Sea during 2018

Igor Yashayaev, Ingrid Peterson, and Zeliang Wang

Fisheries and Oceans Canada
Ocean and Ecosystem Sciences Division
Bedford Institute of Oceanography
P.O. Box 1006, 1 Challenger Drive
Dartmouth, Nova Scotia B2Y 4A2

Canada

Foreword

This series documents the scientific basis for the evaluation of aquatic resources and ecosystems in Canada. As such, it addresses the issues of the day in the time frames required and the documents it contains are not intended as definitive statements on the subjects addressed but rather as progress reports on ongoing investigations.

Correct citation for this publication:

Yashayaev, I., Peterson, I., and Wang, Z. 2021. Meteorological, Sea Ice, and Physical Oceanographic Conditions in the Labrador Sea during 2018. DFO Can. Sci. Advis. Sec. Res. Doc. 2021/042. iv + 26 p.

Aussi disponible en français :

Yashayaev, I., Peterson, I., et Wang, Z. 2021. Conditions météorologiques, état de la glace de mer et propriétés physiques de l'eau dans la mer du Labrador en 2018. Secr. can. de consult. sci. du MPO. Doc. de rech. 2021/042. iv + 30 p.

TABLE OF CONTENTS

ABSTRACT

In the Labrador Sea, wintertime surface heat losses result in the formation of dense waters that play an important role in ventilating the deep ocean and driving the global ocean overturning circulation. In the winter of 2017–18, as in the previous two winters, the subpolar North Atlantic experienced below-average (2017–18) to average (2015–16 and 2016–17) surface heat losses, which were significantly lower than the 2014–15 winter heat loss, that was the highest since 1993–94. The winter (December–March) North Atlantic Oscillation (NAO) index in 2017–18, and winter ocean-atmosphere heat fluxes, in the central Labrador Sea, were near their long-term average values. However, atmospheric circulation, associated with a high atmospheric pressure anomaly extending throughout the Labrador Sea in winter, resulted in above-normal air and sea surface temperatures in the western Labrador Sea, and below-normal temperatures in the northeastern Labrador Sea. For sea surface temperature, these conditions persisted into the spring season, appearing to propagate cyclonically. Sea ice concentration anomalies in February and March, 2018, were generally negative in the western Labrador Sea, and positive in the northeastern Labrador Sea, consistent with the atmospheric circulation and air temperature anomalies. The upper 100 m layer of the central Labrador Sea has been cooling since 2010. However, the intermediate (200–2000 m) layer only started to cool after 2011, which was the layer's warmest year during 1972–2018. This cooling was mainly caused by ongoing deepening of winter convection. Indeed, despite a reduction in the cumulative heat losses from the sea surface after 2014–15, the depth of winter convection continued to increase in the three winters that followed. This is mainly due to the water column preconditioning caused by convective mixing in the previous years. The multiyear persistence of deepening winter convection (eventually exceeding 2000 m in depth) has resulted in the most voluminous, densest and deepest formation of Labrador Sea Water since 1994. Bedford Institute of Oceanography North Atlantic model simulations suggest that the transport of the Labrador Current decreased between 1995 and 2014, but has since increased slightly.

INTRODUCTION

The Labrador Sea is located between Greenland and the Labrador coast of Eastern Canada. Its deep, semi-enclosed basin is bounded by the West Greenland and the Newfoundland-Labrador shelves. Cold, low-salinity waters of polar origin circle the Labrador Sea in a counterclockwise current system that includes both the northward flowing West Greenland Current (WGC) on the eastern side and the southward flowing Labrador Current (LC) on the western side (Figure 1). Much warmer and saltier patches of water can be found under the offshore extensions of the WGC and LC. These are variations of the Atlantic Water originating in the low latitudes of the Atlantic Ocean, following first the North Atlantic Current and then the Gulf Stream. As the Atlantic Water flows into and around the Labrador Sea, following its eastern, northern and eventually western boundaries, it mixes with other masses, progressively cooling and freshening.

Spatial distribution and temporal changes in temperature, salinity, density, dissolved oxygen, and other environmental variables, in the upper and deep layers of the Labrador Sea, respond to a wide range of external and internal oceanic factors. The external factors include: exchanges with land (e.g., continental runoff) and atmosphere (e.g., radiation); latent and sensible heat, and momentum fluxes; precipitation; evaporation; and exchanges with other substances (such as anthropogenic gases). The internal factors include: inflows of warmer and saltier waters from the adjacent North Atlantic; inflows of colder and fresher waters from the Arctic; and local oceanic processes, such as lateral mixing and winter convection. Naturally, the physical, chemical and biological properties throughout the sea (both horizontally and vertically) are subjected to seasonal, interannual, and decadal variations in the affecting factors. In addition, instantaneous conditions and process development depend on the cumulative effect of past heat, salt, and freshwater gains and respective temperature, salinity, and density changes, termed as ocean preconditioning (Yashayaev and Loder 2017).

Since 1990, the Bedford Institute of Oceanography (BIO) has been conducting annual occupations of the oceanographic section Atlantic Repeat 7-West (AR7W). This section, spanning the Labrador Sea (Figure 1, Table 1), was first included as both one-time (A1E) and repeat (AR7W) hydrographic lines in the World Ocean Circulation Experiment (WOCE) array (Lazier et al. 2002; Kieke and Yashayaev 2015; Yashayaev et al. 2015). Later, the observations collected on the AR7W line became, and presently remain, an important contribution of Canada to the international Global Climate Observing System (GCOS), the Climate Variability (CLIVAR) component of the World Climate Research Programme (WCRP), and the Global Ocean Ship-based Hydrographic Investigations Program (GO-SHIP).

The annual multidisciplinary survey of AR7W is presently recognized as the core component of the Atlantic Zone Off-shelf Monitoring Program (AZOMP) of Fisheries and Oceans Canada (DFO), and has been highlighted in numerous high-impact publications (e.g., Thornalley et al. 2018; Lozier et al. 2019; Fröb et al. 2016; Holliday et al. 2020), special journal issues (e.g., Progress in Oceanography, Vol. 73, 3–4, 2007; Progress in Oceanography, Vol. 132, 2015; Yashayaev et al. 2015; Kieke and Yashayaev 2015), and books (e.g., Arctic-Subarctic Ocean Fluxes: Defining the Role of the Northern Seas in Climate, 2008).

Section AR7W spans approximately 900 km from Misery Point, Labrador, to Cape Desolation, Greenland. Because of heavy sea-ice conditions in some years, the shelf stations cannot always be reached and, hence, the shelves are more limited in data coverage than the deep basin and even the slope region. With nearly three decades of annual surveys, the time series now allows an examination of multiyear trends in all key ecosystem variables. Only one year, 2017, was missed in the 30-year long history of the occupations of the AR7W line by BIO. Since

1995, the mid-point date of the survey has occurred between early May and late July, with the earliest dates occurring since 2014, and the latest dates occurring before 2004 (Table 1). For biological variables, the variability in survey date provides information on the seasonal cycles in different regions (Fragoso et al. 2016). For physical variables, the variability in survey date has a significant effect near the surface (0–100 m), but little effect at depths greater than 200 m. In any case, the seasonal cycle has been removed for all depths in this report, in order to provide information on the interannual variability of the physical variables, both near the surface and at depth.

Additionally, the scope of AZOMP activities includes occupations of the Extended Halifax line (XHL, Figure 1), maintaining deep-water oceanographic moorings in the Labrador Sea and on the Scotian Slope and deployments of profiling Argo floats in both regions.

METEOROLOGICAL OBSERVATIONS

NORTH ATLANTIC OSCILLATION (NAO) INDEX

The NAO is an important teleconnection pattern influencing atmospheric processes in the Labrador Sea (Barnston and Livezey 1987; Hauser et al. 2015). When the NAO is in its positive phase, low-pressure anomalies over the Icelandic region and throughout the Arctic, combined with high-pressure anomalies across the subtropical Atlantic, produce stronger-than-average westerlies across the mid-latitudes. Conditions over the northwestern Atlantic, including the Labrador Sea region, are colder and drier than average. A negative NAO indicates weakening of both the Icelandic low and Azores high, which decreases the pressure gradient across the North Atlantic, resulting in weakening of the westerlies and brings warmer conditions than usual. Both NAO phases are associated with basin-wide changes in the intensity and location of the North Atlantic jet stream and storm track, and in large-scale modulations of the zonal and meridional heat and moisture transport (Hurrell 1995), resulting in the modification of the temperature and precipitation patterns. Even though the focus of this report is on the past seven decades, we analyze the entire 122-year long record of instrumental NAO observations to relate the recent conditions to the major shifts in the atmospheric situations over the North Atlantic.

NAO index anomalies (relative to the 1981–2010 mean) computed using two versions of the NAO index are shown in Figure 2 (upper panel). The station-based NAO index (green) is the difference in winter (December, January, February, March) sea-level, atmospheric pressure between the Azores and Iceland (Hurrell et al. 2018). The PC-based NAO index (blue) is associated with the first Empirical Orthogonal Function (EOF) of standardized monthly 500-mb height anomaly fields for the Northern Hemisphere. The spatial pattern of this EOF shows a high over southern Greenland, and a low near the latitude of the Azores.

The wintertime NAO exhibits significant multi-decadal variability (Hurrell 1995). An upward trend of the NAO index from the 1960s to the 1990s was noted by Visbeck et al. (2001), although since the peak in the 1990s there has been a slight downward trend. Recent studies reveal an atmospheric circulation pattern, complementary to NAO, which becomes more prominent in years of low NAO (Hauser et al. 2015). Further study of this phenomenon will help to improve understanding and forecasting capabilities of atmospheric and oceanic conditions.

In 2010, the NAO index reached a record low (Figure 2, upper panel). In 2011, the NAO index rebounded from the record low but still remained well below the 30-year average (1981–2010). In 2012, however, the NAO index was strongly positive, up to a level comparable to those in early 1990s showing the highest winter index over the last twenty years. There was a significant change in the winter NAO index in 2013, when it became moderately negative. In 2014, the NAO index returned to its high positive phase, slightly lower than the 2012 value, making it the

second highest in the last twenty years. In 2015 there was another high NAO event, the largest positive NAO magnitude in the 122-year long instrumental record. In 2017, the winter NAO index was slightly positive in both versions but significantly smaller than in 2012, 2015, and even 2016. In 2018, the station-based NAO anomaly (green) was slightly negative, while the PC-based NAO anomaly (blue) was weakly positive. In both cases, the NAO has decreased from the extremely high values observed in 2015.

Figure 2 also shows a map of Sea Level Pressure (SLP) anomalies in winter 2018 (December, January, February, March) over the North Atlantic, relative to the 1981–2010 mean. A large high-pressure anomaly can be seen extending from Davis Strait southward past the Azores. This pattern would be associated with stronger-than-normal southerly winds on the western side of the Labrador Sea, and northerly winds on the eastern side.

AIR TEMPERATURES

The air temperature data used are from the National Centers for Environmental Prediction (NCEP) Reanalysis dataset, provided by the NOAA/OAR/ESRL PSD, Boulder, Colorado, USA. The NCEP Reanalysis is a joint project between the National Centers for Environmental Prediction and the National Center for Atmospheric Research (NCAR). The goal of this joint effort is to produce a new Surface Air Temperature and Sea Surface analysis, using historical data (1948 onwards), and to produce analyses of the current atmospheric state (Kalnay et al. 1996).

Time series plots of winter and spring air temperature anomalies in the Labrador Basin (55 to 60°N, 50.0 to 52.5°W) are shown in Figure 3, and winter and spring maps of surface air temperature anomalies in 2018 from the NCEP Reanalysis are shown in Figure 4. In the winter map, a high positive anomaly can be seen on the western side of the Labrador Sea, and a negative anomaly on the eastern side, consistent with the SLP anomalies noted in the previous section.

AIR-SEA HEAT FLUX

The cumulative air-sea heat flux integrated over individual-year cooling seasons (cumulative winter surface heat flux/loss in Figures 3 and 9) was computed using 6-hourly heat flux and daily-mean radiation data obtained from the U.S. NCEP Reanalysis (Kalnay et al. 1996). The two available versions of NCEP Reanalysis products, R1 and R2, are jointly used to provide the most extensive up-to-date data coverage.

The total or cumulative surface heat loss incurred in a cooling season was estimated by integrating the net surface heat flux over the Labrador Basin from start to end of the cooling period. The net heat flux values used in this integration were computed as a sum of incoming and outgoing shortwave and longwave radiative, and latent and sensible turbulent heat flux components extracted for the region of interest from the NCEP/NCAR Reanalysis fields. The start and end points of each cooling cycle were associated with the net flux reversals in fall and spring (Yashayaev and Loder 2009).

The highest annual heat losses during 1974–2018 were achieved in 1993 and 2015. Since 1998, the top six cumulative surface heat losses have occurred in 2008, 2012, 2014, 2015, 2016, and 2017.

REMOTELY-SENSED SEA SURFACE TEMPERATURE (SST)

The sea surface temperature data used are from the NOAA Optimum Interpolation (OI) Sea Surface Temperature (SST) V2. NOAA_OI_SST_V2 dataset provided by the NOAA/OAR/ESRL

, Boulder, Colorado, USA. The OISST analysis is constructed by combining observations from satellites, ships, and buoys on a regular global grid, and interpolating to fill in gaps.

Time series plots of winter and spring sea surface temperature anomalies in the Labrador Basin (55–60°N, 50.0–52.5°W) are shown in Figure 3. Winter and spring maps of sea surface temperature anomalies (Figure 5) show similar patterns to the air temperature anomalies. In the winter map, warm anomalies can be seen over most of the Labrador Sea, and a cold anomaly off southwestern Greenland. In spring, the cold anomaly appears to propagate westward across the Northern Labrador Sea.

SEA ICE OBSERVATIONS

Sea ice concentrations derived from satellite passive microwave data since late 1978 are obtained from the U.S. National Snow and Ice Data Center. These data were used instead of Canadian Ice Service data because they extend farther east, so that they cover the Greenland Shelf—comparisons show that the anomalies computed from each dataset for the same area agree very close.

Monthly sea ice concentration data are used for 1978–2017 (Cavalieri et al. 1996, Fetterer et al. 2002) and daily real-time data are used for 2018 (Meier et al. 2017). Ice extent is defined as the area in which ice concentration is at least 15%, and is computed for three latitude bands in the Labrador Sea region: 63–68°N (Davis Strait), 58–63°N (Northern Labrador Sea), and 53–58°N (Labrador Shelf).

Winter and spring time series of sea ice extent anomalies for these three regions are shown in Figure 6. Winter and spring ice extent anomalies in 2018 are positive for Davis Strait, but spring anomalies are near-normal for the Northern Labrador Sea, and Labrador Shelf.

Figure 7 shows monthly maps of sea ice concentration anomalies (top panel) and extent (bottom panel) in January to March 2018, using data from the US National Snow and Ice Data Center. The magenta lines in the lower panel show the median limit of ice extent. Off western Greenland in February and March, positive ice concentration anomalies can be seen, and the ice extent is higher than normal, in agreement with winter air temperature and sea surface temperature anomalies. In the western Labrador Sea, sea ice concentration is generally below normal, and ice extent is generally near-normal or below-normal.

OCEAN TEMPERATURES AND SALINITIES

SHIPBOARD OBSERVATIONS

Since 2004, the AR7W survey has been carried out mostly in May with at least 30 Conductivity-Temperature-Depth (CTD)—although a broader range of sensors than these three are used routinely on every AZOMP mission—and water sampling (e.g., for dissolved oxygen, nutrients, transient tracer) stations occupied between Labrador and Greenland. The pressure, temperature, conductivity, salinity, and dissolved oxygen data sets have been quality controlled and calibrated to meet WOCE standards, using water sample (e.g., Autosal salinity and Winkler titration), SBE35 temperature recorder and laboratory calibration data. Argo float temperature and salinity profiles, available since 2002, have been quality controlled through comparisons with vessel CTD and water sample data and comparisons between floats, and by performing critical analyses of spatial and temporal deviations. The historical and other recent data have also been quality controlled and processed through similar critical analyses. See Yashayaev and Seidov (2015) for a summary of the data editing and processing approaches used here as well.

The AZOMP and past BIO Labrador Sea data are enhanced and expanded by adding publically available observed-level temperature and salinity data archived by other programs and national and international data centers (e.g., Kieke and Yashayaev 2015).

ARGO PROFILING FLOAT DATA

Argo is an international network of profiling floats collecting high-quality temperature and salinity profiles from the upper 2000 m of the ice-free global ocean, and through float displacements, currents from intermediate depths. For most of a typical 10-day cycle, a battery-powered autonomous float freely drifts at a "parking depth" of usually 1000 m, where its position is stabilized through buoyancy adjustment. Once the float is released from its parking depth, it descends to approximately 2000 m and then ascends to the surface, while profiling temperature, salinity, and other variables, if additional sensors are installed. When the surface is reached, the acquired data are transmitted, and the float sinks back to its parking depth. Since 2002, the near real-time temperature and salinity Argo float data collectively draw a large-scale picture of the oceanographic structure and circulation of the Labrador Sea. The array is typically used to reconstruct the seasonal and interannual variability of the physical characteristics and dissolved oxygen in the upper 2000 m water column. The value of the Argo floats is even more significant in winter, when they serve as the only means of providing information about real-time development of winter convection, and when there are no shipboard measurements available.

Overall, the network of profiling Argo-floats-provided temperature and salinity data to 2000 m is used for monitoring of year-round variability of the oceanographic conditions in the Labrador Sea. However, the number of the floats within the Labrador Sea during 2018 was just marginally sufficient to resolve sub-monthly variability.

SYNTHESIS OF MULTIPLATFORM DATA SETS

Temperature and salinity data in the Labrador Sea from various sources are compiled and seasonally adjusted to provide individual time series. Our primary data sources include *(i)* full-depth temperature, salinity, and dissolved oxygen profiles collected on the AR7W line across the Labrador Sea that has been occupied by BIO in support of WOCE, CLIVAR and recently AZOMP since 1990, *(ii)* water sample and discrete temperature data used to calibrate the instrument sensors, *(iii)* temperature and salinity profiles over the upper 2000 m in the Labrador Sea region from the International Argo float program, *(iv)* publically available observed-level temperature and salinity data from other programs and national and international data centers (e.g., Kieke and Yashayaev 2015), and *(v)* a near-bottom moored temperature time series from a long-term mooring maintained by the BIO on the Labrador Slope.

The main data additions to the previous years are observations from Argo floats up to March 2019 and DFO's annual CTD survey of the AR7W line across the Labrador Sea in May 2018 (Figure 1).

Following Yashayaev and Loder (2009, 2016 and 2017), but now including all available Argo and ship-based survey data to March 2019, time-depth series of spatially averaged potential temperature, salinity, and potential density with weekly-to-monthly (dependent on Argo and ship survey data coverage) resolution have been computed for an area of approximately 60,000 km^2 in the central Labrador Sea.

For each depth level included in a chosen depth layer, a time series has been compiled with all individual CTD, water sample, and Argo measurements (profiles) of an analyzed variable within the central Labrador Sea. The measurements have been corrected, depth by depth, for seasonality (wherever applicable), by using an iterative procedure, obtaining a harmonic representation of the seasonal cycle and removing data outliers. The resulting series have been

low-pass-filtered, and the filtered values have been averaged annually to obtain the annual variable values since 1987.

Further, to place the recent variability in a historical context, we use annual time series of temperature, salinity, and density averaged over the 15–100 and 200–2000 m vertical intervals in the central Labrador Sea, back to 1948, as long-term indices of these variables over its upper and intermediate-depth waters. These were derived from time series for selected depths like those discussed above and previously reported.

WINTER CONVECTION AND HYDROGRAPHIC CONDITIONS IN THE CENTRAL LABRADOR SEA

LONG-TERM CHANGES IN KEY WATER MASSES

Multidecadal time-depth distributions of annual temperature, salinity, and density in the central Labrador Sea since 1950 at depths of 200–3500 m are shown in Figure 8. The intermediate, deep, and abyssal (or bottom) water masses found in the Labrador Sea are Labrador Sea Water (LSW), Northeast Atlantic Deep Water (NEADW, 2500–3000 m), and Denmark Strait Overflow Water (DSOW, defined as a 200 m thick bottommost layer at the water depths exceeding 3000 m). Similarly to DSOW, NEADW is also derived from the Iceland-Scotland Overflow Water, but it undergoes a longer and more substantial mixing, transformation, and modification along its path (Yashayaev and Dickson 2008).

While the temporal changes within NEADW are comparably slow, typically spanning a few decades, and appear to be vertically-uniform (note how NEADW salinity changed 1975 to 2001 to present in Figure 8), both LSW and DSOW exhibit strong variations on decadal and shorter time scales. Recurring warm and saline, and cold and fresh events, spread in the upper 2000 m layer mainly occupied by LSW. A period characterized by warming and salinification of this layer, that started in the mid-1960s and ended in the early or mid-1970s, was followed by a period with opposite trends in temperature and salinity, signified by cooling and freshening of LSW, culminated in the late 1980s to mid-1990s. This period was characterized by deep, winter convection that filled the upper 2000–2500 m layer of the Labrador Sea with cold, dense, and relatively fresh water. Milder winters in the early 2000s produced more limited amounts of LSW, which have gradually become warmer, saltier, and less dense than in the previous decade (Yashayaev 2007).

Time series plots of annual, spring, and May temperature and salinity, at depths of 15–100 m and 200–2000 m, are presented in Figure 9. Both upper (15–100 m) and deeper (200–2000 m) layers have been cooling since 2010. However, the freshening trend seen in the newly-formed or newly-ventilated LSW between 2011 and 2016, reversed in 2016, making the LSW formed in the winter of 2017–18 the densest since the mid-1990s.

Also shown in Figure 9 are the winter NAO and cumulative winter surface heat flux (because the ocean loses heat through each cooling season, this metric can also be regarded as cumulative heat loss). Their low-pass filtered values (centered on the last year of the filter window) represent the combined effect of recent surface heat losses and water column preconditioning in previous years.

RECENT SEASONAL AND INTERANNUAL VARIABILITY IN THE UPPER 2000 M

Time-depth distributions of monthly temperature, salinity, and density at depths of 0–2000 m since 2002 (when Argo floats became widespread) are presented in Figure 10. The positive temperature and negative density trends established in the top 1000 m of the sea, following the

cessation of extreme convection in the mid-1990s, were repeatedly interrupted by moderately deep convection in the winters of 1999–2000, 2001–2002 (Figure 8), 2007–2008, and 2011–2012 (Figures 8 and 10). These particularly long temperature and density trends kept reestablishing themselves after each interruption, resuming nearly the same directions and rates they had before the interruption. However, despite their multiyear persistence, the aforementioned trends reversed their directions to sustained cooling and density increase in the winter of 2013–14, when deep convection reaching to 1500 m of depth and below, spanned a considerable part of the Labrador Basin. Deep convection has deepened progressively over the five consecutive winters (2013–14 through 2017–18). During this period, each convective development produced a colder, denser, and deeper LSW than the preceding event. As result, the convectively formed water mass, LSW, was getting colder and denser as convection deepened between 2014 and 2018, inclusively. Overall, the progressive cooling of the top 2000 m, and deep and intense winter mixing during the five consecutive winters of 2013–14 through 2017–18, have interrupted the general warming and stratification-building trend that has persisted in the intermediate waters of the Labrador Sea since the mid-1990s.

The deep convection event of 2007–08 is evident in both the temperature and salinity fields. The depth of shallower convection in 2008–09 was partly reduced because of massive surface freshening in the preceding summer and fall. The conditions in the winter of 2010–11 were similar to those in the preceding winter, with very limited convection (mixed layer depths did not exceed 800 m). Then, in the winter of 2011–12, convection reached the depths of approximately 1400 m, which is clearly present in temperature and salinity profiles acquired by both Argo floats and ship survey. Salinity in the top 200 m in 2012 was the lowest since 2003, particularly in the top 50 m. Convection also occurred in the winter of 2012–13, but it was not as deep as in the previous year, and was mostly limited to the top 1000 m. The situation changed quite significantly in the winter of 2013–14. Wintertime cooling triggered convective mixing, homogenizing the top 1600 m (and probably even deeper) layer in the central Labrador Sea. Winter convection progressed over the following four years, reaching deeper and making the top 2000 m layer colder and denser with every cooling cycle. In the last of these winters, convection reached and exceeded the depth of 2000 m. These very persistent recent trends in temperature (negative), density (positive), and convection depth (positive), evident in Figures 8 to 10, support our earlier supposition that a multiyear recurrence of relatively strong cooling, typically backed by high NAO, results in convective preconditioning of the water column in such a way that an even deeper convection may occur in a following year, even under milder cooling conditions. Indeed, in the winter of 2017–18, as in the previous two winters, the subpolar North Atlantic basins lost considerably less heat to surface cooling than in the winter of 2014–15 (that demonstrated the highest cumulative surface heat loss in more than two decades). The cumulative 2017–18 winter heat loss in the Labrador Sea was also the lowest since the winter of 2013–14. Despite the continual reduction in winter cooling, the steady increase in the depth of winter convection since 2014–15 has resulted in the development of the most significant class of LSW, in terms of volume, depth, and density, since 1994.

The persistence in deep convective mixing contributing to the massive LSW development in the recent years is effectively shown in the temporal progression of cascading vertical temperature, salinity, and density profiles (Figure 10), as the cold dense water reaches deeper and deeper with time. Each of the freshly-made, deepened, and densified LSW vintages was in part preserved in the deep basin until the next winter. This illustrates the essence of water column preconditioning by winter convection – sustaining or "memorizing" the previous year conditions throughout the intermediate depths at the convection site.

In addition to surface heat flux, another factor that could potentially change convection is surface freshening due to accelerated melting of the Greenland Ice Sheet. However, a recent

study by Dukhovskoy et al. (2019) indicates that the effect of the Greenland freshwater flux anomaly produced by the observed acceleration of Greenland Ice Sheet melt is not sufficient to fully explain the present changes in water-column salinity and convective activity. In fact, there is no significant negative trend present in surface salinity in the Labrador Basin in the last decade.

2017–18 WINTER CONVECTION HIGHLIGHTS

The monthly temperature and salinity data (Figure 10) show that the winter mixed layer, and hence convection, in the central Labrador Sea reached and even exceeded 2000 m in March of 2018, continuing the trend of the winter-mixed-layer deepening of the last seven years. The recent increment in convection depth supports our earlier explanation of sustained multiyear deepening of winter convection. With respect to 2018, it implies that certain extreme properties, such as low temperature, weak vertical stability, and weak overall stratification, imposed on the water column by the stronger-than-usual convective mixing in the previous years, had resulted in a preconditioning that has facilitated further development of deep convection (Figures 8–10, the successive deepening of winter mixing is clearly visible in Figure 10).

Distance-depth plots of temperature, salinity, density, and oxygen from the survey data in 1994, 2011, and 2018 are presented in Figure 11. A reservoir filled with this newly ventilated, 2000 m deep, cold, dense, fresh, atmospheric-gas-loaded LSW is clearly evident in the AR7W seawater property section based on shipboard CTD data collected in the 2018 May AZOMP survey. The 2018 vintage of LSW is associated with low temperature (< 3.3°C) and low salinity (< 34.86) between 1000 and 2000 m. The winter convection in the recent time period, 2015–2018, especially in the winter of 2017–18, is arguably the deepest since the record-deep cooling that reached 2400 m in the winter of 1993–94. The present LSW year class is one of the largest ever observed outside of the early 1990s.

CALCULATIONS FROM NUMERICAL SIMULATION MODEL

In this report, an ocean model hindcast from the Bedford Institute of Oceanography North Atlantic Model (BNAM) is used to calculate the variations of the Labrador Current, and the variations of its two branches as well (details in the section of Results and Discussion). The BNAM is based on the NEMO (Nucleus for European Modelling of the Ocean) 2.3 model. It includes an ocean component OPA (Océan Parallélisé) and a sea ice module LIM (Louvain-la-Neuve Sea Ice Model). The barotropic transport is used to represent the strength of the current. The hindcast period is from 1990 to 2018. This portion of our report is intended to demonstrate changes of the currents and their potential representation of the Atlantic Meridional Overturning Circulation (AMOC).

The BNAM model domain was selected to include the North Atlantic Ocean (7ºN–75ºN and 100ºW–25ºE) with a nominal resolution of 1/12º. The model has a maximum of 50 levels in the vertical, with level thickness increasing from 1 m at the surface to 200 m at a depth of 1250 m and reaching the maximum value of 460 m at the bottom of the deep basins. The maximum depth represented in the model is 5730 m.

Open boundary data are from the GLORYS reanalysis product (Global Ocean ReanalYses and Simulations). The model surface forcing is taken from a combination of CORE (Coordinated Ocean-ice Reference Experiments) and NCEP/NCAR reanalysis forcing. Model forcing variables include: air temperature; wind velocities and humidity; daily short- and long-wave radiation; and total precipitation (rain plus snow). No surface restoring to sea-surface temperature is applied. However, the model's sea-surface salinity is restored to its monthly climatology with a 60-day restoring time scale.

The model was spun-up for 10 years using the CORE normal year forcing. The 10-year spin-up simulation is initialized with a January climatology of temperature and salinity (T-S). The T-S climatology combines the Polar Science Center Hydrographic Climatology (PHC2.1) at high latitudes with the T-S climatology of WOA5 (World Ocean Atlas 2005) at middle and low latitudes.

For the purposes of the present report, the transports were calculated based on modelled flows through the western segment of the AR7W transect.

VARIATIONS OF THE LABRADOR CURRENT

The variations of the Labrador Current (LC) can be seen as an indicator for the changes in the subpolar, North Atlantic circulation, the region of which plays an important role in the global climate due to the winter convection event in the Labrador Sea. The variations of the LC are often connected to the variations of the AMOC. Here we present the variations of barotropic transports of the LC from an eddy-resolving model developed at Bedford Institute of Oceanography (BNAM, e.g., Brickman et al. 2016; Wang et al. 2016; Brickman et al. 2018; Wang et al. 2018).

An EOF analysis of the model output by Wang et al. (2016), presented in Figure 12, suggests the variability in the Labrador Current can be partitioned into a western Labrador Current (WLC; from the 300–2500 m isobaths), and an eastern Labrador Current (ELC; from the 2500–3300 m isobaths). Following the definition of the WLC and ELC, we calculated the transports of ELC and WLC, and also those of the LC (the summation of the ECL and WLC).

Figure 13 shows the transport anomalies for the LC, ELC and WLC. The WLC in 2018 was marginally stronger than in 2017, about 2 Sv above the 1990–2018 mean, as it has been since 2001.

A declining trend of the ELC began in 1996, coinciding with a significant drop in the winter NAO index in the same year. The trend reversed in 2014, and the ELC was approximately 4 Sv stronger in 2018 than in 2017, although still remaining approximately 2 Sv below the 1990–2018 average. Wang et al. (2016) suggested that the ELC is an indicator for the changes in the AMOC, which would imply a possible significant weakening followed by a strengthening of the AMOC since 2014 based on the BNAM hindcast.

SUMMARY

The Atlantic Zone Off-Shelf Monitoring Program (AZOMP) of Fisheries and Oceans Canada provides observations of variability in the ocean climate and ventilation. The changes observed by the program are closely linked to the dynamics of the planetary climate system as a whole and affect the regional climate and ecosystems off Atlantic Canada. In May of 2018, the AR7W line was occupied by the Bedford Institute of Oceanography for the thirty-first time since 1990. Additionally, the network of profiling Argo floats provided temperature and salinity data (to 2000 m) used for monitoring of year-round variability of the oceanographic conditions in the Labrador Sea. An omission of a single year (as 2017) in precise systematic observations of the ocean state can significantly limit our ability to diagnose and predict the state of the ocean, making us rely exclusively on profiling float, remote-sensed, and atmospheric reanalysis data when assessing coast-to-coast full-depth environmental conditions in the key ocean's region.

Key characteristics of the past and recent environmental conditions in the Labrador Sea are summarized in the scorecard shown in Figure 14, and are listed below:

1. The winter (December to March) NAO index in 2018 was above-normal, while the average winter heat fluxes in the central Labrador Sea was near-normal. However, a high atmospheric pressure anomaly extended throughout the Labrador Sea in winter, resulting in above-normal air and sea surface temperatures in the western Labrador Sea, and below-normal temperatures in the northeastern Labrador Sea. For SST, these conditions persisted into the spring, but appeared to have propagated cyclonically.

2. Sea ice concentration anomalies in February and March of 2018 were generally negative in the western Labrador Sea, and positive in the northeastern Labrador Sea. For the Davis Strait region, winter and spring ice extent anomalies in 2018 were positive. For the Northern Labrador Sea and Labrador Shelf regions, ice extent anomalies were negative in winter and near-normal in spring.

3. Ocean temperature in the central Labrador Sea was near-normal and continued a negative trend observed since 2010 in the 15–100 m layer, and, since 2011, in the 200–2000 m layer. The cooling of the deeper layer was primarily caused by deepening of winter convection.

4. In the Labrador Sea, surface heat losses in winter result in the formation of dense waters, which spread across the ocean, ventilating its deep layers and essentially driving the global ocean-overturning circulation. In the winter of 2017–18, as in the previous two winters (2015–16 and 2016–17), the subpolar North Atlantic experienced a more moderate surface heat loss than in the winter of 2014–15 that featured the highest heat losses in more than two decades.

5. Despite the persistent decline in the surface cooling after the winter of 2014–15, the water column preconditioning by convective mixing, that had progressed over the four years preceding 2018, led, nevertheless, to the most significant formation in terms of volume and depth, of Labrador Sea Water (LSW) since 1994.

6. The temperature and salinity profiles obtained by the ship survey and Argo floats show that the winter mixed layer, and hence convection in the central Labrador Sea, penetrated below 2000 m in 2018, exceeding the mixed layer depths of 1600 m, 1700 m, 1850 m, and 1900 m observed in 2014, 2015, 2016, and 2017, respectively. The 2018 vintage of LSW is associated with low temperature (<3.3°C) and salinity (<34.86) between 1000 m and 1900 m. The winter convection developed in the last five years (2014–2018) or, if excluding 2013, seven years (2014–2018), is arguably the deepest since the record of 2500 m in 1994; while the resulting LSW year-class is one of the largest ever observed outside of the first pentad of the 1990s. This also suggests that the strong winter convection in the winter of 2017–18 further added to increased gas (dissolved oxygen, anthropogenic gases, and carbon dioxide) uptake, and consequently, respective gas concentrations in the Labrador Sea in the lower part of the 0–2000 m layer.

7. Model results suggest that the transport of the Labrador Current decreased between 1995 and 2014, but has since increased slightly.

REFERENCES CITED

Barnston, A. G., and Livezey, R. E. 1987. Classification, seasonality and persistence of low-frequency atmospheric circulation patterns. Mon. Wea. Rev.115: 1083–1126.

Brickman, D., Wang, Z., and Detracy, B. 2016. Variability of Current Streams in Atlantic Canadian Waters: A Model Study. Atmosphere-Ocean. 54 (3): 218–229.

Brickman, D., Hebert, D., and Wang, Z. 2018. Mechanism for the recent ocean warming events on the Scotian Shelf of eastern Canada. Cont. Shelf Res. 156: 11–22.

Cavalieri, D. J., Parkinson, C.L., Gloersen, P., and Zwally, H.J. 1996. updated yearly. Sea Ice Concentrations from Nimbus-7 SMMR and DMSP SSM/I-SSMIS Passive Microwave Data, Version 1. [north/monthly]. Boulder, Colorado USA. NASA National Snow and Ice Data Center Distributed Active Archive Center. [Accessed 05/12/2018].

Dickson, R. R., Meincke, J. and Rhines, P. (Eds). (2008) Arctic-Subarctic Ocean Fluxes: Defining the Role of the Northern Seas in Climate, Edited by, Springer Science & Business Media, March 4, 2008, 736 pages.

Dukhovskoy, D. S., Yashayaev, I., Proshutinsky, A., Bamber, J. L., Bashmachnikov, I. L., Chassignet, E. P., Lee C. M., and Tedstone, A. J. 2019, Role of Greenland Freshwater Anomaly in the Recent Freshening of the Subpolar North Atlantic, Journal of Geophysical Research: Oceans. 124 (5): 3333–3360.

Fetterer, F., Knowles, K., Meier, W. and Savoie, M. 2002. Updated 2011. Sea ice index. Boulder, CO: National Snow and Ice Data Center. Digital media.

Fragoso, G.M., Poulton, A.J., Yashayaev, I., Head, E.J.H., Stinchcombe, M., and Purdie, D.A. 2016. Biogeographical patterns and environmental controls of phytoplankton communities from contrasting hydrographical zones of the Labrador Sea, Progress in Oceanography. 141: 212–226.

Fröb, F., Olsen, A., Våge, K., Moore, K., Yashayaev, I., Jeansson, E., and Rajasakaren, B. 2016. Irminger Sea deep convection injects oxygen and anthropogenic carbon to the ocean interior. Nature Communications.13244.

Hauser, T., Demirov, E., Zhu, J., and Yashayaev, I. 2015. North Atlantic atmospheric and ocean inter-annual variability over the past fifty years – Dominant patterns and decadal shifts. Progress in Oceanography. 132: 197–219.

Holliday, N.P., Bersch, M., Berx, B., Chafik L., Cunnningham, S., Florindo-Lopez, C., Hatun, H., Johns, W., Josey, S.A., Larsen, K. M. H., Mulet, S., Oltmanns, M., Reverdin, G., Rossby, T., Thierry, V., Valdimarsson, H. and Yashayer, I. 2020. Ocean circulation causes the largest freshening event for 120 years in eastern subpolar North Atlantic. Nature Communications. 11: 585.

Hurrell, J.W. 1995. Decadal trends in the North Atlantic Oscillation: Regional temperatures and precipitation. Science. 269: 676–679.

Hurrell, J. W. and National Center for Atmospheric Research Staff Eds. (Last modified 04 Aug 2018). The Climate Data Guide: Hurrell North Atlantic Oscillation (NAO) Index (station-based).

Kalnay, E., Kanamitsu, M., Kistler, R., Collins, W., Deaven, D., Gandin, L., Iredell, M., Saha, S., White, G., Woollen, J., Zhu, Y., Chelliah, M., Ebisuzaki, W., Higgins, W., Janowiak, J., Mo, K.C., Ropelewski, C., Wang, J., Leetmaa, A., Reynolds, R., Jenne, R., and Joseph, D. 1996. The NCEP/NCAR 40-Year Reanalysis Project., Bull. Amer. Meteor. Soc. 77 (3): 437–470.

Kieke, D., and Yashayaev, I. 2015. Studies of Labrador Sea Water formation and variability in the subpolar North Atlantic in the light of international partnership and collaboration, Progress in Oceanography. 132: 220–232.

Lazier, J. R. N., Hendry, R. M., Clarke, R. A., Yashayaev, I., and Rhines, P. 2002. Convection and restratification in the Labrador Sea, 1990–2000, Deep Sea Res., Part A. 49: 1819–1835.

Lozier, M.S., et al., 2019. A sea change in our view of overturning in the subpolar North Atlantic, Science. 363 (6426): 516–521.

Meier, W. N., Fetterer, F., and Windnagel, A. K. 2017. *Near-Real-Time NOAA/NSIDC Climate Data Record of Passive Microwave Sea Ice Concentration, Version 1*. [north/daily]. [Accessed 05/12/2018].

Progress in Oceanography, 2007, Observing and Modelling Ocean Heat and Freshwater Budgets and Transports, Edited by Igor Yashayaev. 73 (3–4): 203–426.

Progress in Oceanography, 2015, Oceanography of the Arctic and North Atlantic Basins, Edited by Igor Yashayaev, Dan Seidov, Entcho Demirov. 132: 1–352.

Thornalley, D.J.R., Oppo, D.W., Ortega, P., Robson, J.I., Brierley, C.M., Davis, R., Hall, I.R., Moffa-Sanchez, P., Rose, N.L., Spooner, P.T., Yashayaev, I., and Keigwin, L.D. 2018. Anomalously weak Labrador Sea convection and Atlantic overturning during the past 150 years. Nature. 556: 227–230.

Visbeck, M.H., Hurrell, J.W., Polvani, L., and Cullen, H.M. 2001. The North Atlantic Oscillation: Past, Present and Future. Proc. Nat. Acad. Sci. 98: 12876–12877.

Wang, Z., Brickman, D., Greenan, B., and Yashayaev, I. 2016. An abrupt shift in the Labrador Current System in relation to winter NAO events. Journal of Geophysical Research: Oceans. 121: 5338–5349.

Wang, Z., Lu, Y., Greenan, B., Brickman, D., and DeTracey, B. 2018. BNAM: An eddy-resolving North Atlantic Ocean model to support ocean monitoring. Can. Tech. Rep. Hydrogr. Ocean. Sci. 327: vii + 18p.

Yashayaev, I. 2007. Hydrographic changes in the Labrador Sea, 1960–2005, Progress in Oceanography. 73: 242–276.

Yashayaev, I., and Dickson, R. R. 2008. Chapter 21. Transformation and Fate of Overflows in the northern North Atlantic, Arctic-Subarctic Ocean Fluxes: Defining the Role of the Northern Seas in Climate, R.R.Dickson, J.Meincke, P.Rhines (Eds.), Springer ISBN: 978-1-4020-6773-0.

Yashayaev, I., and Loder, J.W. 2009. Enhanced production of Labrador Sea Water in 2008. Geophysical Research Letters. 36 (1).

Yashayaev, I., Seidov, D., and Demirov, E. 2015. A new collective view of oceanography of the Arctic and North Atlantic basins, Progress in Oceanography. 132: 1–21.

Yashayaev, I., and Seidov, D. 2015. The role of the Atlantic Water in multidecadal ocean variability in the Nordic and Barents Seas, Progress in Oceanography. 132: 68–127.

Yashayaev, I., and Loder, J.W. 2016. Recurrent replenishment of Labrador Sea Water and associated decadal-scale variability. Journal of Geophys. Res.: Oceans. 121 (11).

Yashayaev, I., and Loder, J.W. 2017. Further intensification of deep convection in the Labrador Sea in 2016. Geophysical Research Letters. 44 (3).

TABLES

Table 1. Oceanographic Labrador Sea cruises conducted by the Bedford Institute of Oceanography since 1990 as part of WOCE, CLIVAR, AZOMP

| Cruise Name	Vessel	Project	Chief Scientist	Cruise Dates
HUD-92-014	CCGS Hudson	WOCE	John Lazier	27-May to 15-Jun, 1992
HUD-95-011	CCGS Hudson	WOCE	John Lazier	7-Jun to 5-Jul, 1995
HUD-96-006	CCGS Hudson	WOCE	John Lazier	10-May to 2-Jun, 1996
HUD-96-026	CCGS Hudson	WOCE	Allyn Clarke	15-Oct to 20-Nov, 1996
HUD-97-009	CCGS Hudson	WOCE/JGOFS	Allyn Clarke	9-May to 12-Jun, 1997
HUD-98-023	CCGS Hudson	WOCE/CLIVAR	John Lazier	22-Jun to 10-Jul, 1998
HUD-99-022	CCGS Hudson	Climate	Allyn Clarke	27-Jun to 14-Jul, 1999
HUD2000009	CCGS Hudson	Climate	Allyn Clarke	20-May to 8-Jun, 2000
HUD2001022	CCGS Hudson	Climate	Allyn Clarke	30-May to 15-Jun, 2001
HUD2002032	CCGS Hudson	Climate	Allyn Clarke	23-Jun to 19-Jul, 2002
HUD2002075	CCGS Hudson	Biology/Climate	Erica Head	29-Nov to 12-Dec, 2002
HUD2003038	CCGS Hudson	Climate	Allyn Clarke	13-Jul to 4-Aug, 2003
HUD2004016	CCGS Hudson	Climate	Allyn Clarke	14-May to 30-May, 2004
HUD2005016	CCGS Hudson	Climate	Allyn Clarke	27-May to 7-Jun, 2005
HUD2006019	CCGS Hudson	Climate	Ross Hendry	24-May to 8-Jun, 2006
HUD2007011	CCGS Hudson	Climate	Ross Hendry	10-May to 29-May, 2007
HUD2008009	CCGS Hudson	Climate	Glen Harrison	20-May to 4-Jun, 2008
HUD2009015	CCGS Hudson	AZOMP	Glen Harrison	18-May to 1-Jun, 2009
HUD2010014	CCGS Hudson	AZOMP	Glen Harrison	13-May to 30-May, 2010
HUD2011009	CCGS Hudson	AZOMP	Igor Yashayaev	6-May to 29-May, 2011
MLB2012001	CCGS M.L. Black	AZOMP	Igor Yashayaev	25-Jun to 20-Jul, 2012
HUD2013008	CCGS Hudson	AZOMP	Igor Yashayaev	4-May to 28-May, 2013
HUD2014007	CCGS Hudson	AZOMP	Igor Yashayaev	2-May to 26-May, 2014
HUD2015006	CCGS Hudson	AZOMP	Igor Yashayaev	1-May to 26-May, 2015
HUD2016006	CCGS Hudson	AZOMP	Igor Yashayaev	30-Apr to 24-May, 2016
HUD2018008	CCGS Hudson	AZOMP	Igor Yashayaev	25-Apr to 20-May, 2018
AMU2019001	CCGS Amundsen	AZOMP	Igor Yashayaev	2-Jun to 19-June, 2019
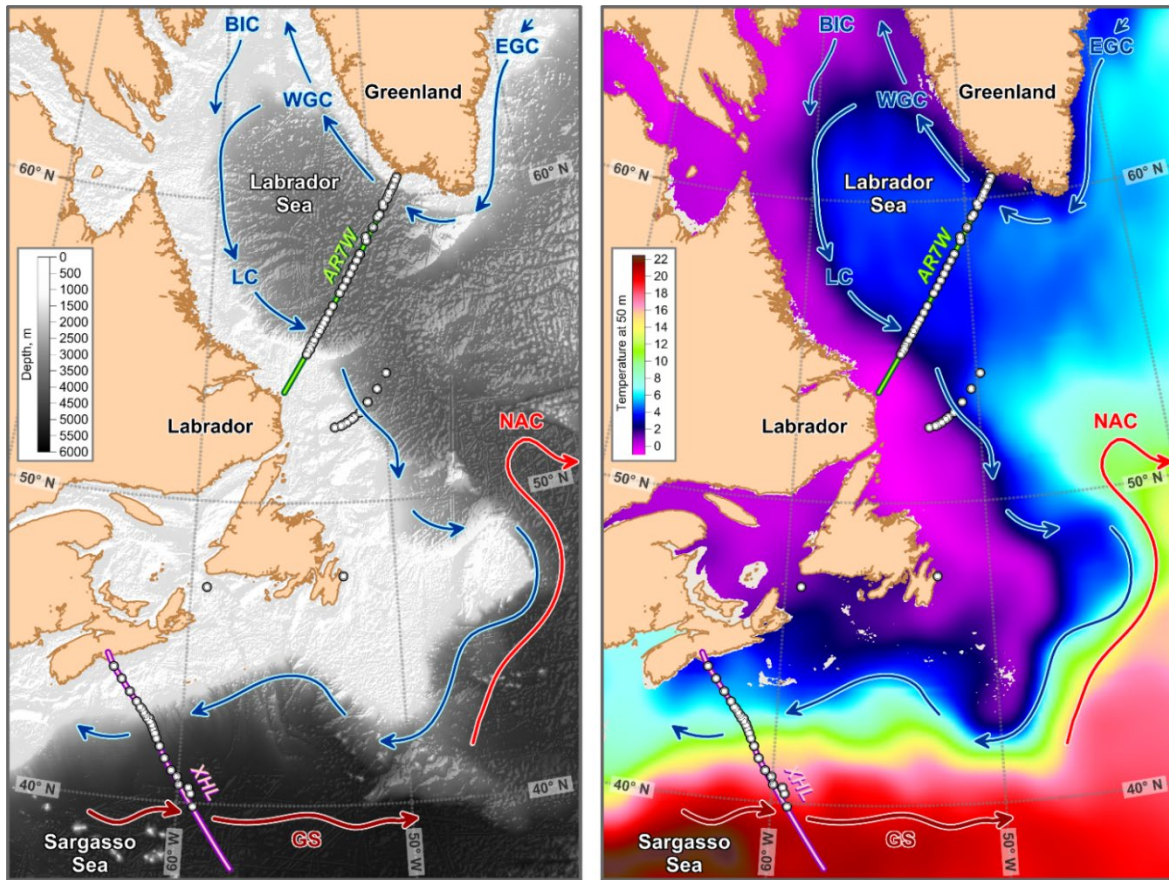
Figure 1. Topography, surface currents (left panel) and long-term mean temperature at 50 m (right panel) in the Atlantic Zone Offshore Monitoring Program (AZOMP) domain. The CTD stations, AR7W and Extended Halifax Lines (XHL) occupied in the 2018 AZOMP mission, HUD2018-008, April 28 to May 24, are shown in both panels.
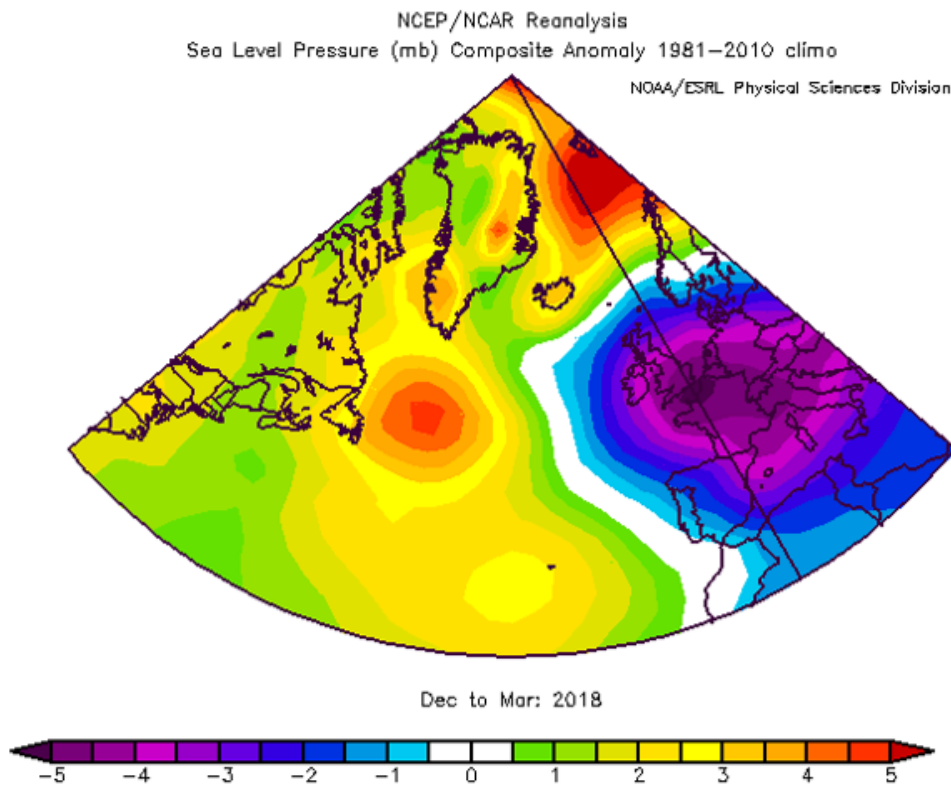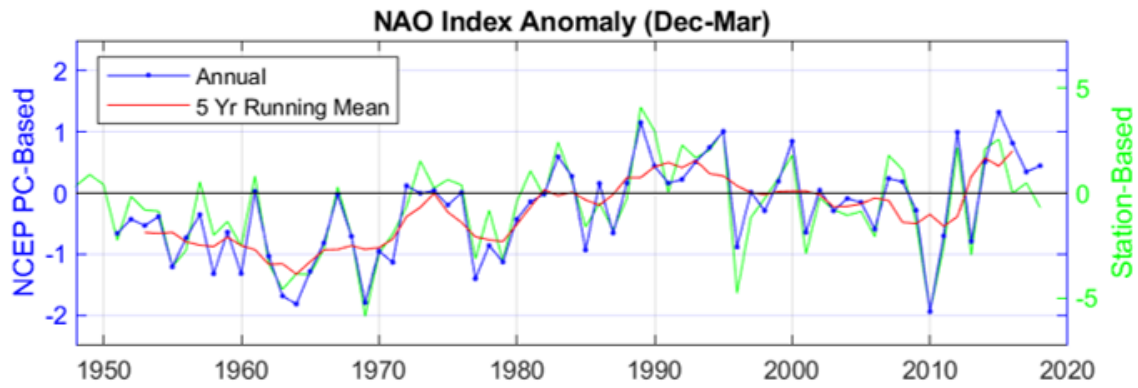
Figure 2. Anomalies of the North Atlantic Oscillation (NAO) index, relative to the 1981–2010 mean. The station-based NAO index (green) is defined as the winter (December, January, February, March) sea level pressure difference between the Azores and Iceland; data were obtained online (Hurrell et al. 2018). The PC-based NAO index (blue) is associated with the first empirical orthogonal function (EOF) of standardized monthly 500-mb height anomaly fields for the Northern Hemisphere; data were obtained online. The lower panel shows the 2018 December–March sea level pressure anomaly over the North Atlantic.
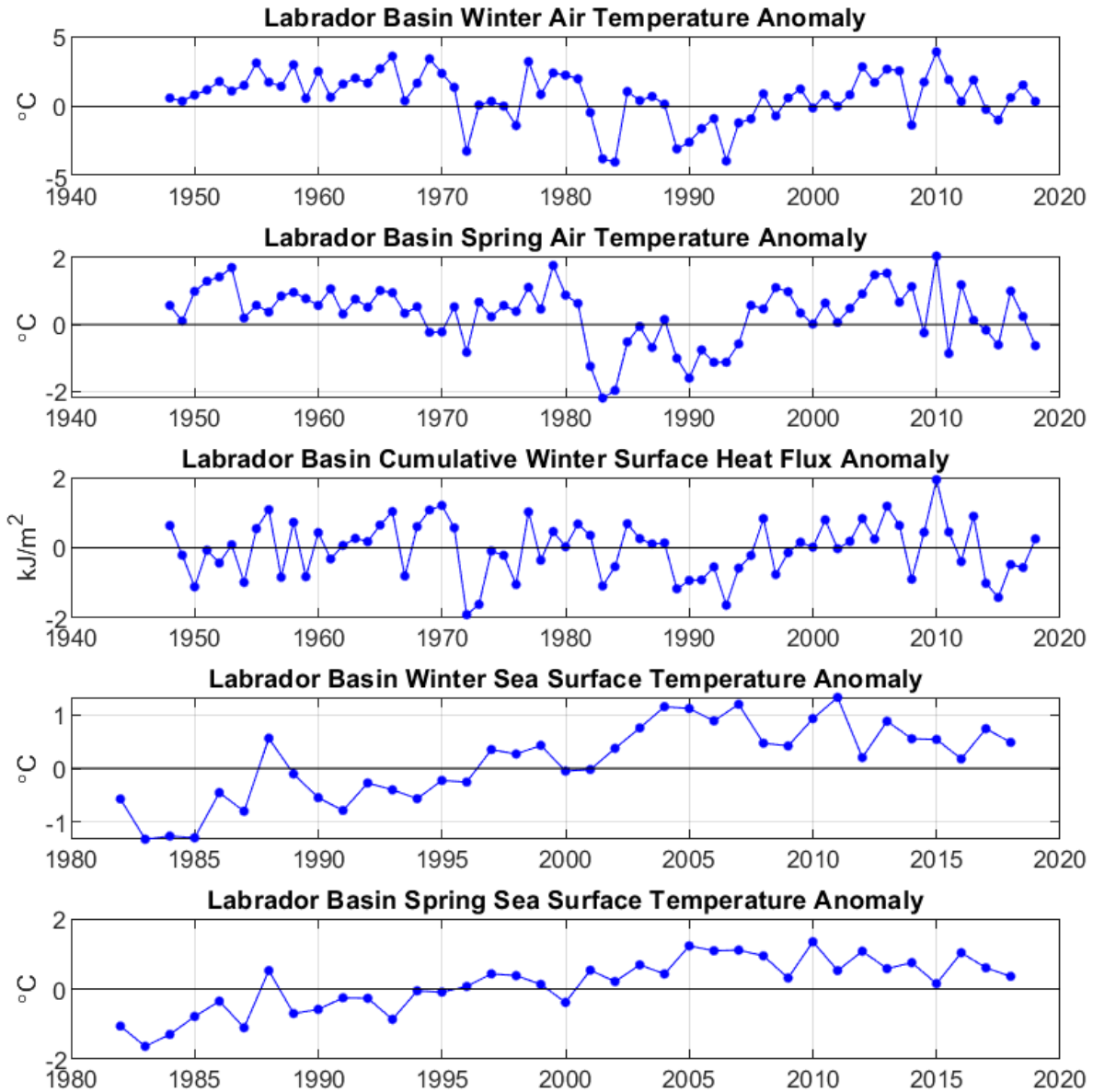
Figure 3. Anomalies of Labrador Basin winter and spring air temperature, cumulative winter surface heat flux, and winter and spring sea surface temperature, relative to the 1981–2010 mean.
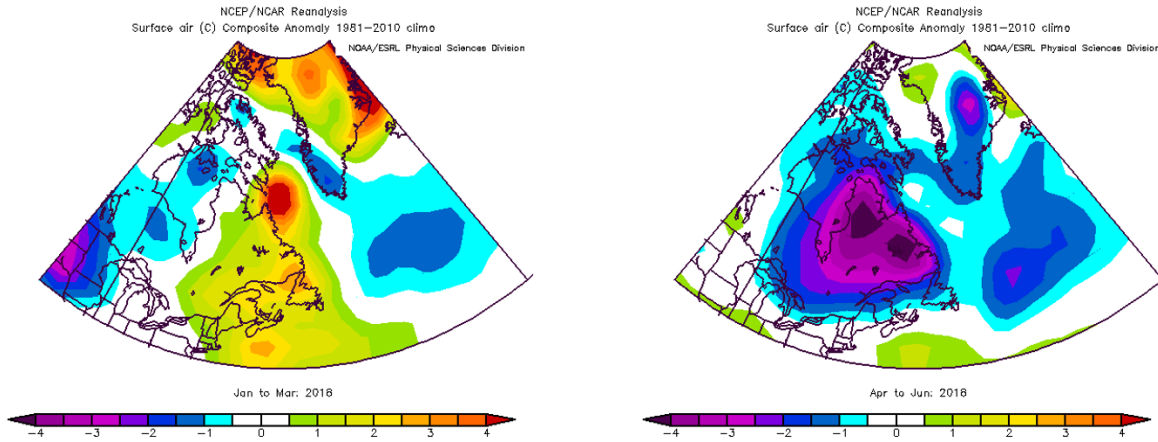
Figure 4. Winter and spring air temperature anomalies (°C) over the Northwest Atlantic relative to the 1981–2010 means; data were obtained from NOAA Internet site (accessed 30 April 2019).
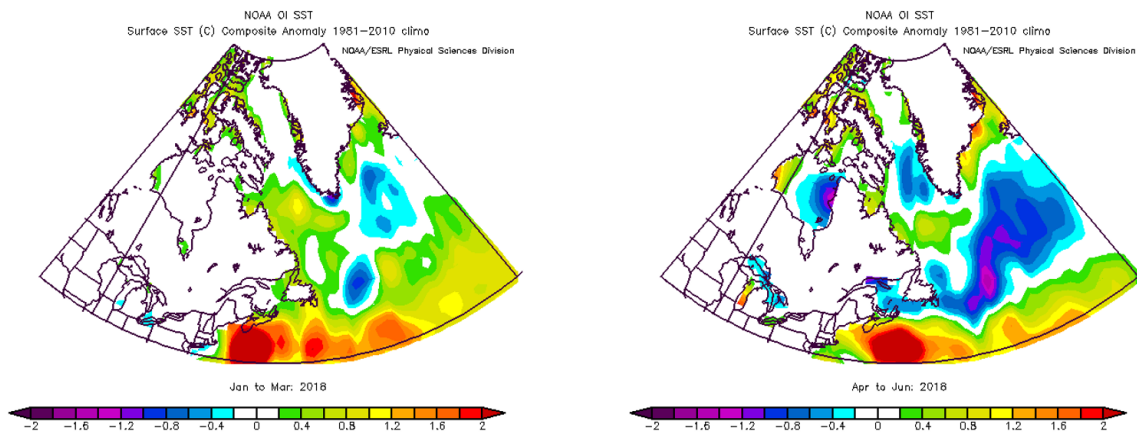
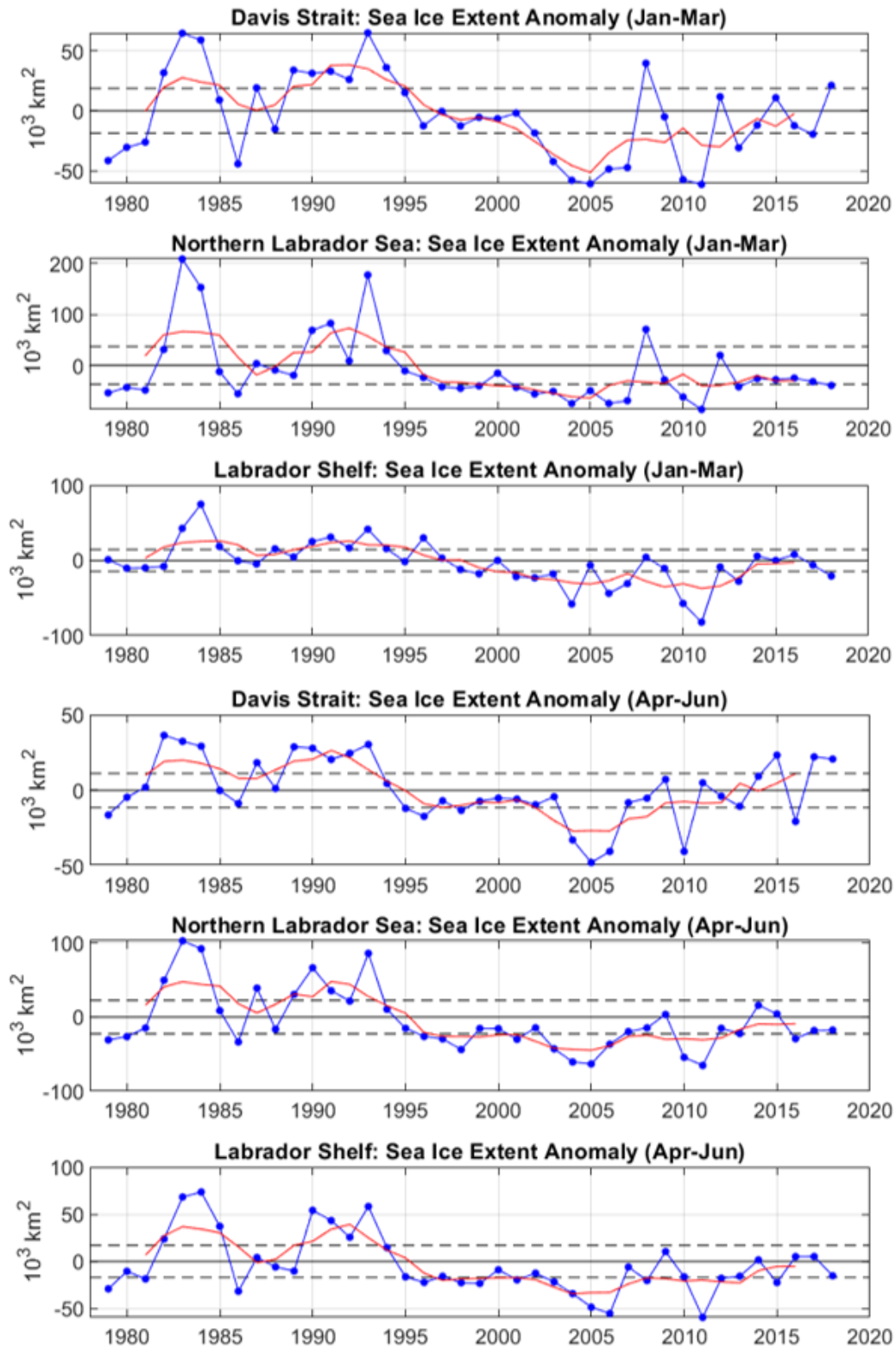*Figure 5. Winter and spring sea surface temperature anomalies (°C) over the Northwest Atlantic relative to the 1981–2010 means; data were obtained from NOAA Internet site (accessed 30 April 2019).*

Figure 6. Winter and spring sea ice extent anomalies (blue) and their five year running means (red) for: (1) Davis Strait (63–68°N), (2) the Northern Labrador Sea (58–63°N), and (3) Labrador Shelf (53–58°N). Horizontal dashed lines represent plus or minus 0.5 SD for the 1981–2010 period.
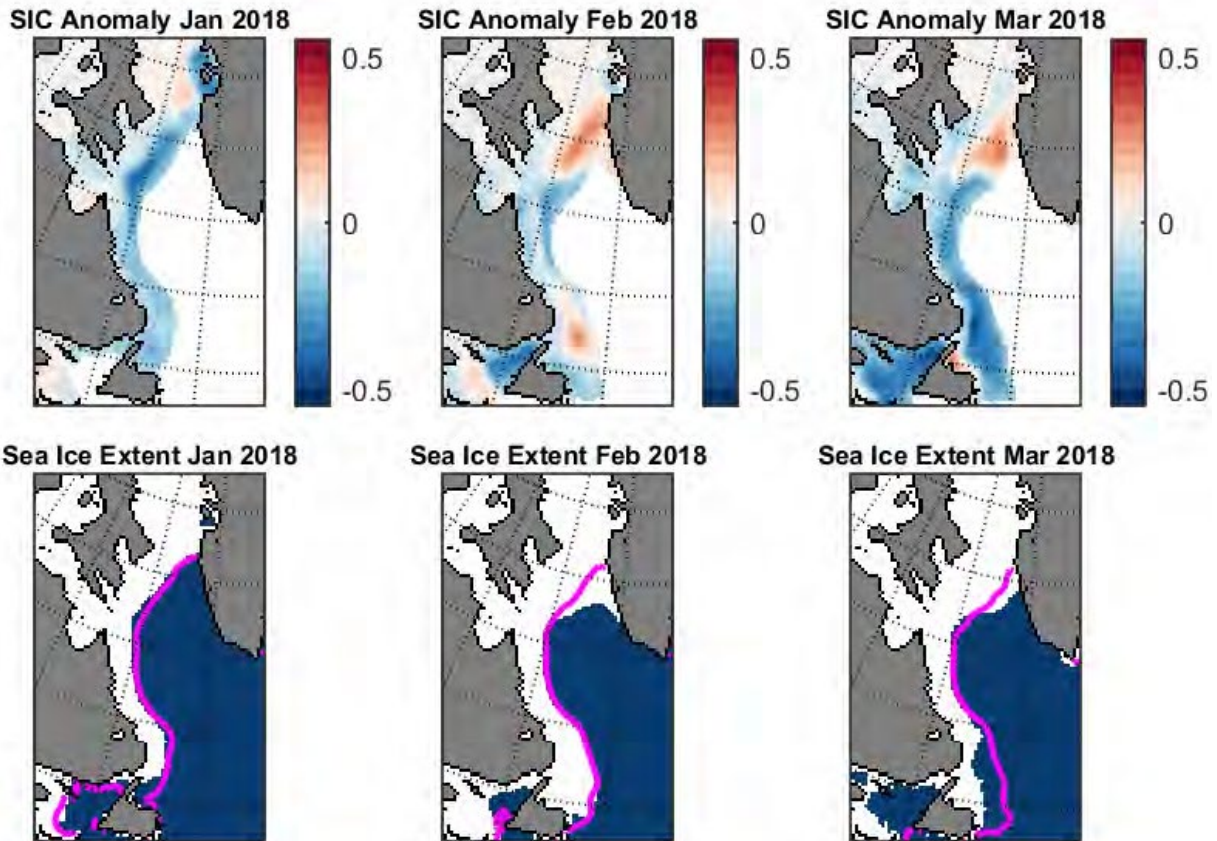
Figure 7. Sea ice concentration anomalies (top) and sea ice extent (bottom) for January–March 2018 as derived by the US National Snow and Ice Data Center (reference period 1979–2000) http://nsidc.org/. The magenta lines show the median ice edge for 1981–2010.
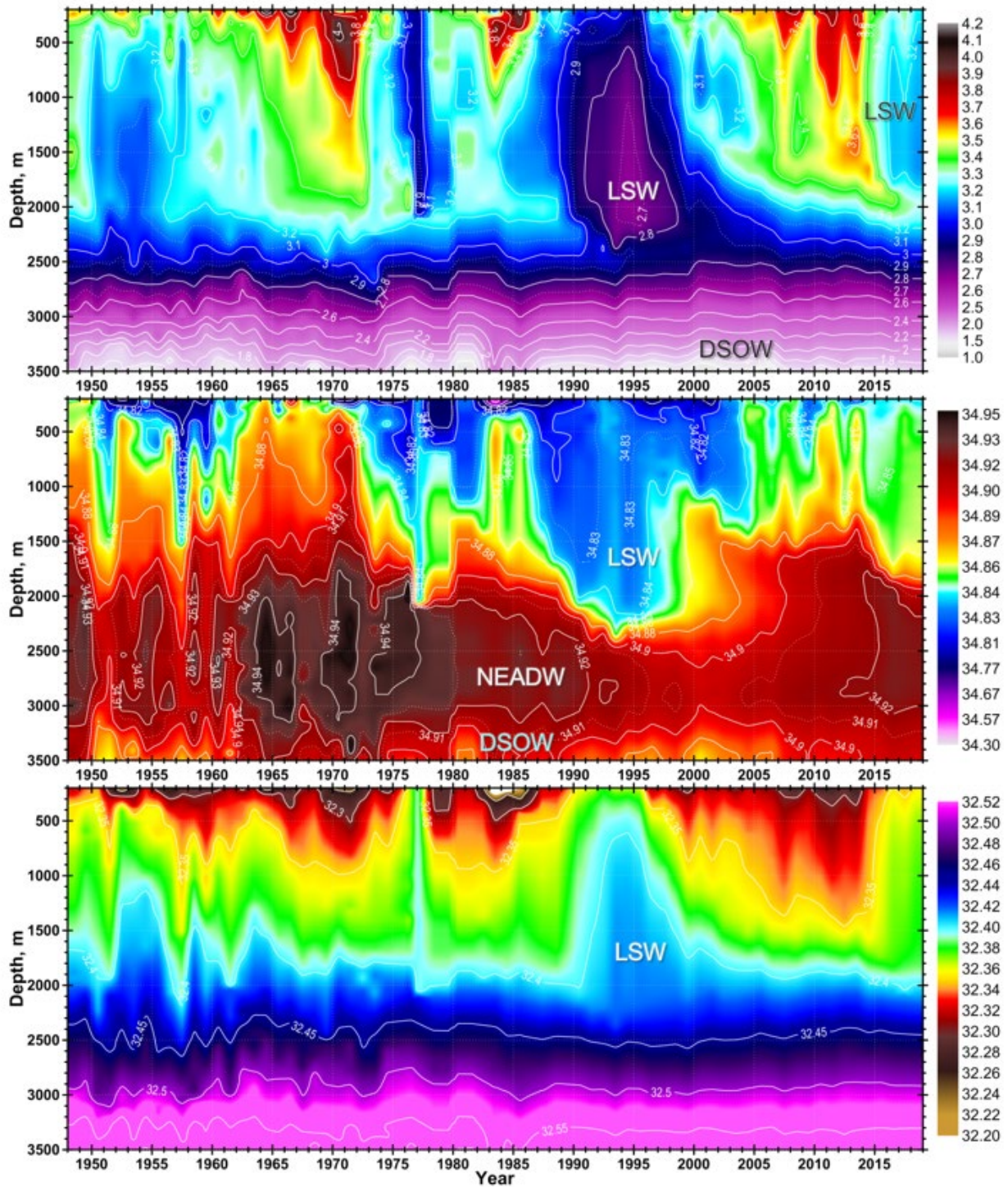
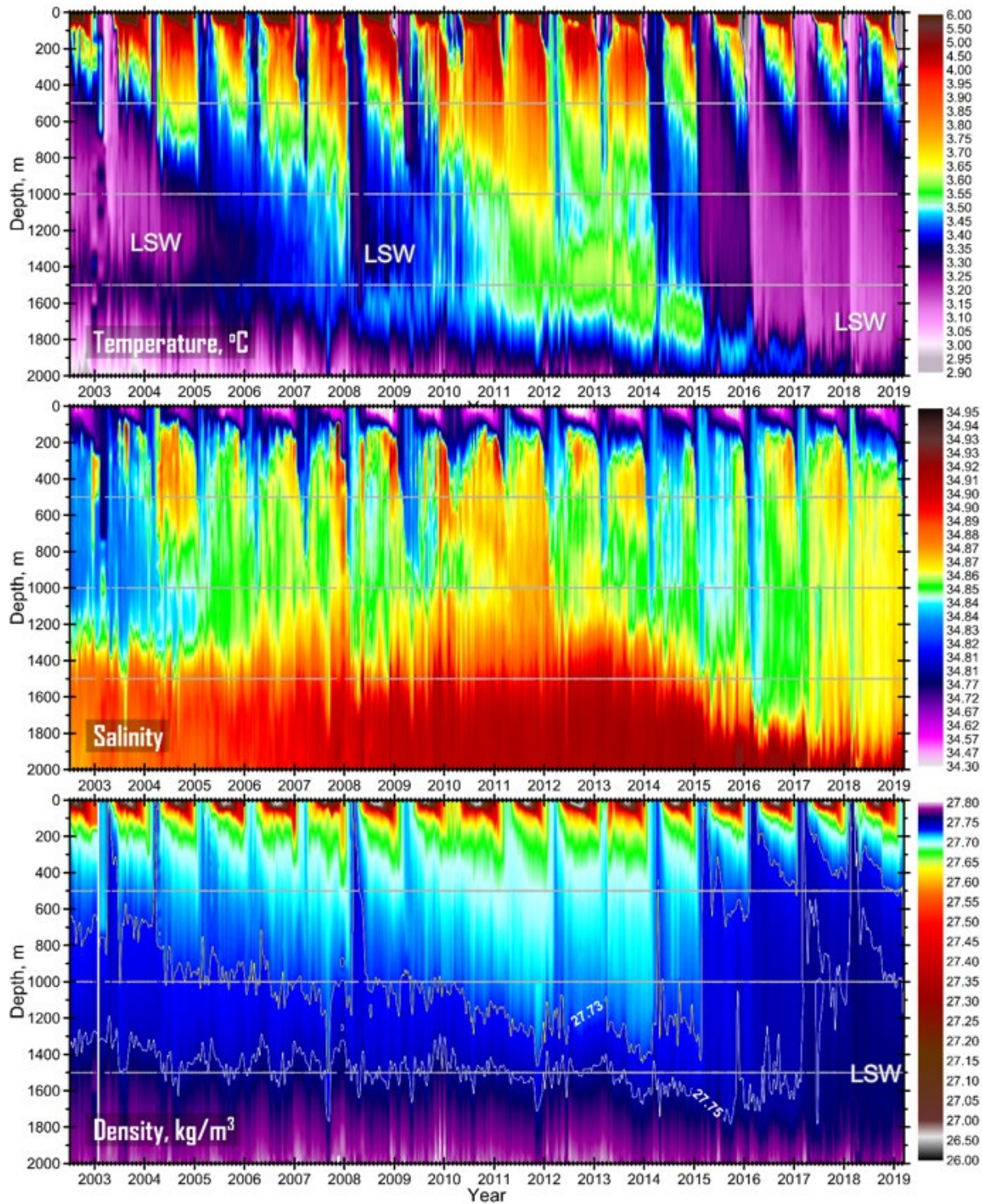*Figure 8. Full water-depth variability of temperature (upper panel), salinity (middle panel) and density (lower panel) in the central region of the Labrador Sea based on profiling Argo float and shipboard observations from 0 m to 2000 m for the time period of 1948–2018. LSW, NEADW and DSOW indicate Labrador Sea Water, Northeast Atlantic Deep Water and Denmark Strait Overflow Water, respectively.*
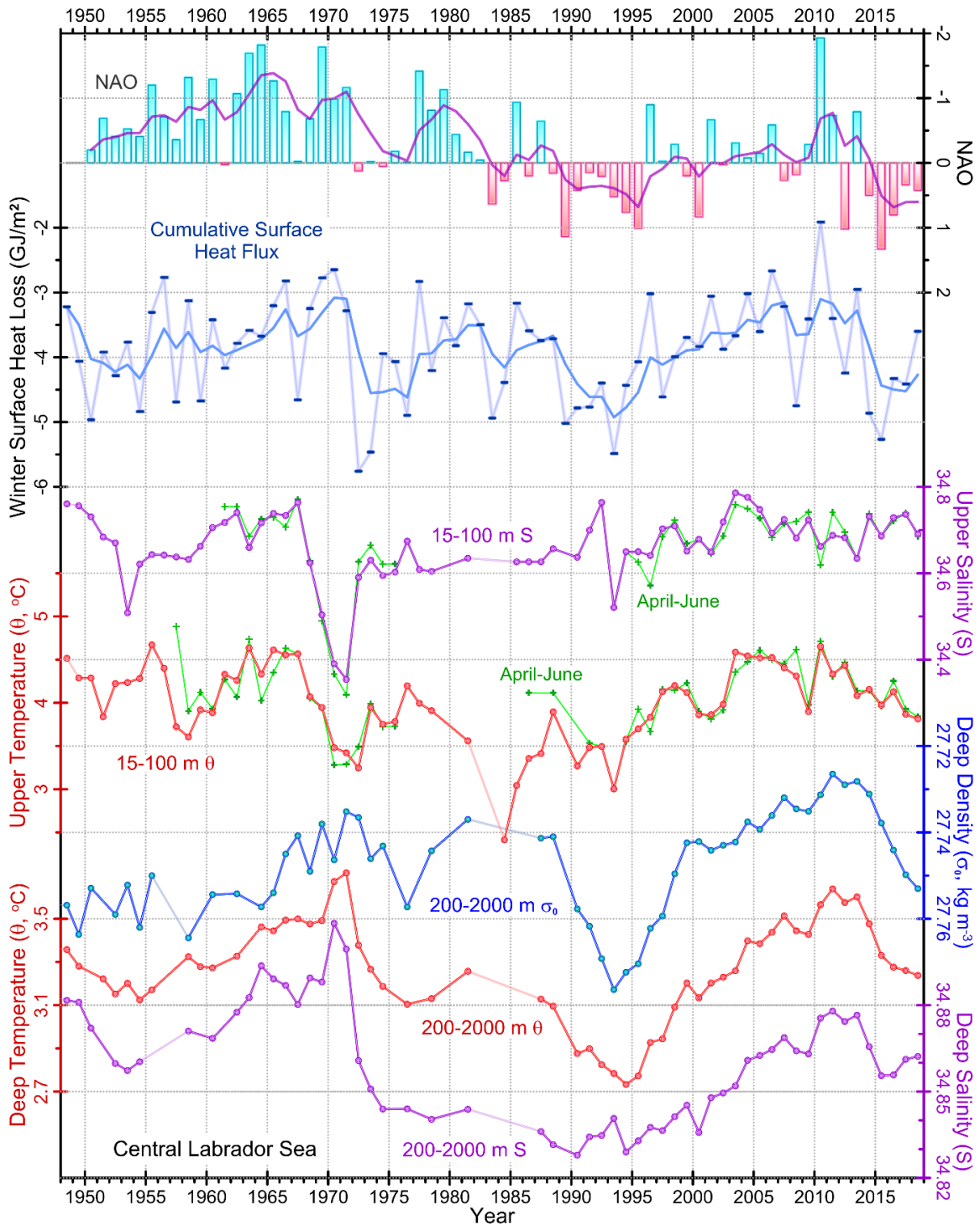
Figure 9. Labrador Sea indices since 1948. From top down: The normalized winter NAO index (upper bar graph, inverted scale); The NCEP-based cumulative surface heat flux computed for the central Labrador Sea over individually-defined annual cooling seasons (blue); The upper two solid lines indicate five-back-point filtered series; Annual and spring mean temperature (θ) and salinity (S) averaged over the 15–100 m depth range, and annual mean θ, S and density (σ$_0$) averaged over the 200–2000 m depth range in the central Labrador Sea.

Figure 10. Variability of temperature (upper panel), salinity (lower panel) and density (middle panel) in the central region of the Labrador Sea based on profiling Argo float and research vessel survey data from 0 m to 2000 m for the time period of 2002–2019.
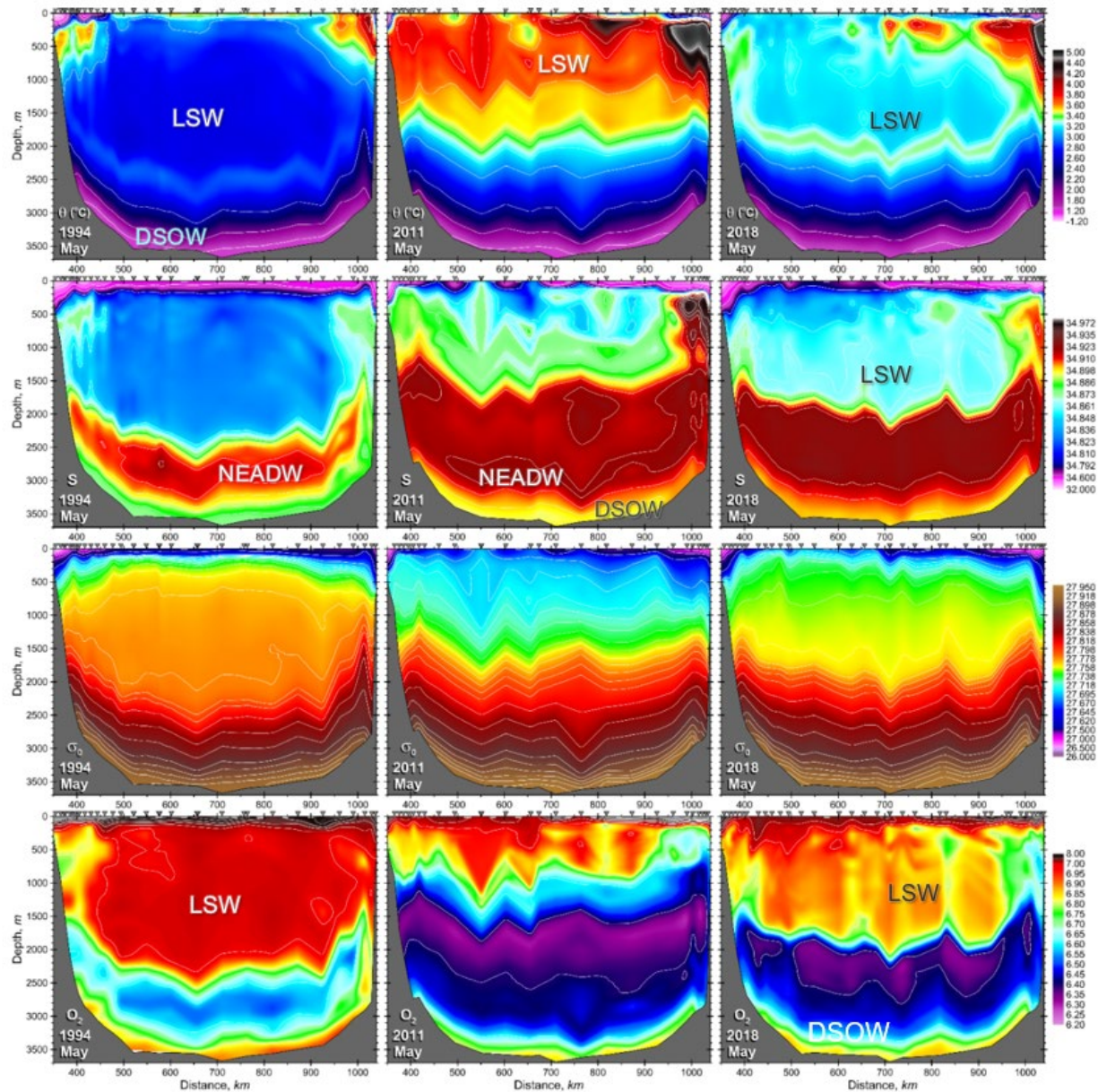
Figure 11. Distributions of potential temperature (θ, °C), salinity (S), potential density (σ₀, referenced to the sea surface, kg/m³) and dissolved oxygen (ml/l) on the AR7W line across the Labrador Sea from annual spring-summer surveys in 1994, 2011 and 2018. Inverted triangles along the top of each panel indicate station locations. LSW, NEADW and DSOW indicate Labrador Sea Water, Northeast Atlantic Deep Water and Denmark Strait Overflow Water, respectively.
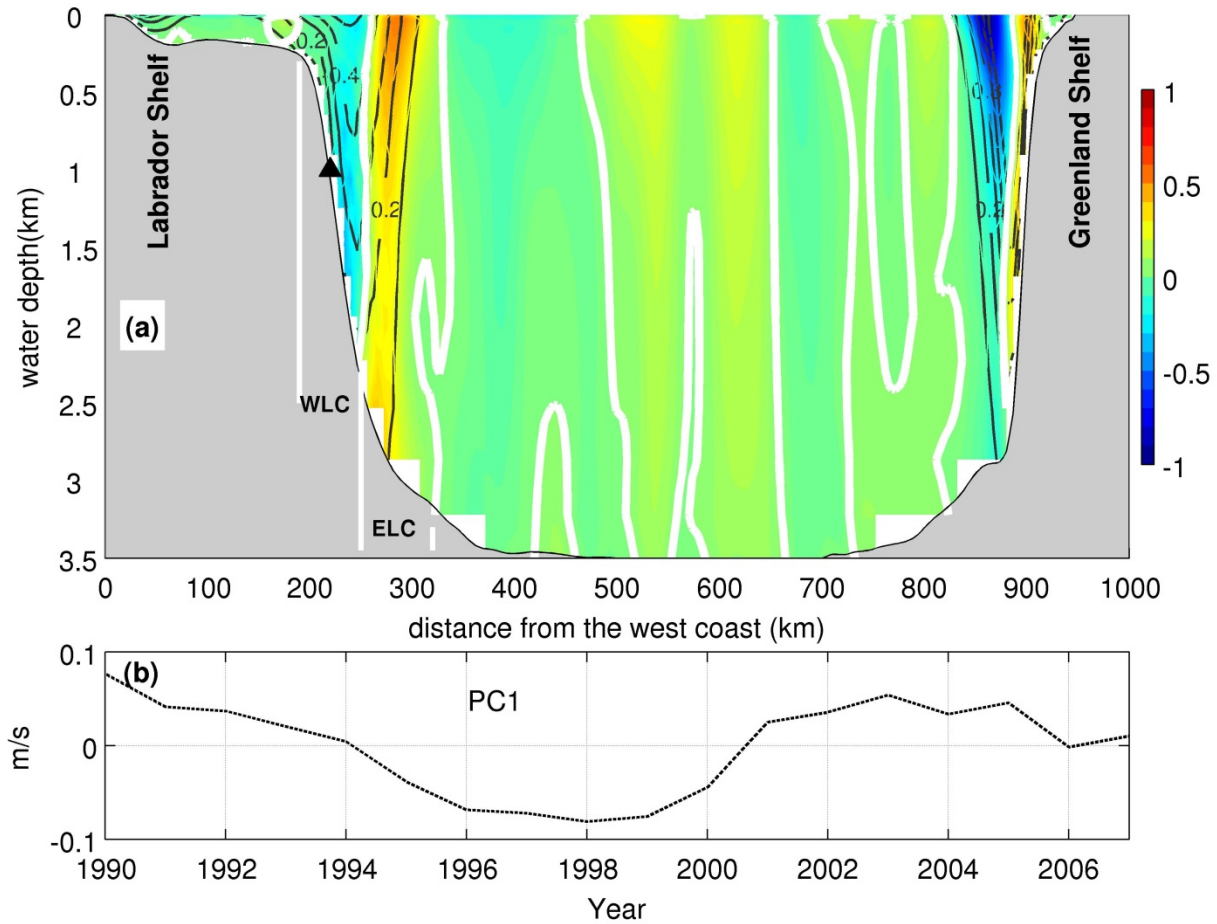
Figure 12. (a) EOF1 pattern of the normal velocities along AR7W (based on results from 1990 to 2007). The shaded areas represent the EOF pattern, bold white lines are zeros contours of the EOF pattern, the black labeled lines are the mean normal velocities (in m/s). Note: positive direction is northward. The black triangle indicates the location of the mooring referred to in the text. (b) Corresponding PC1.
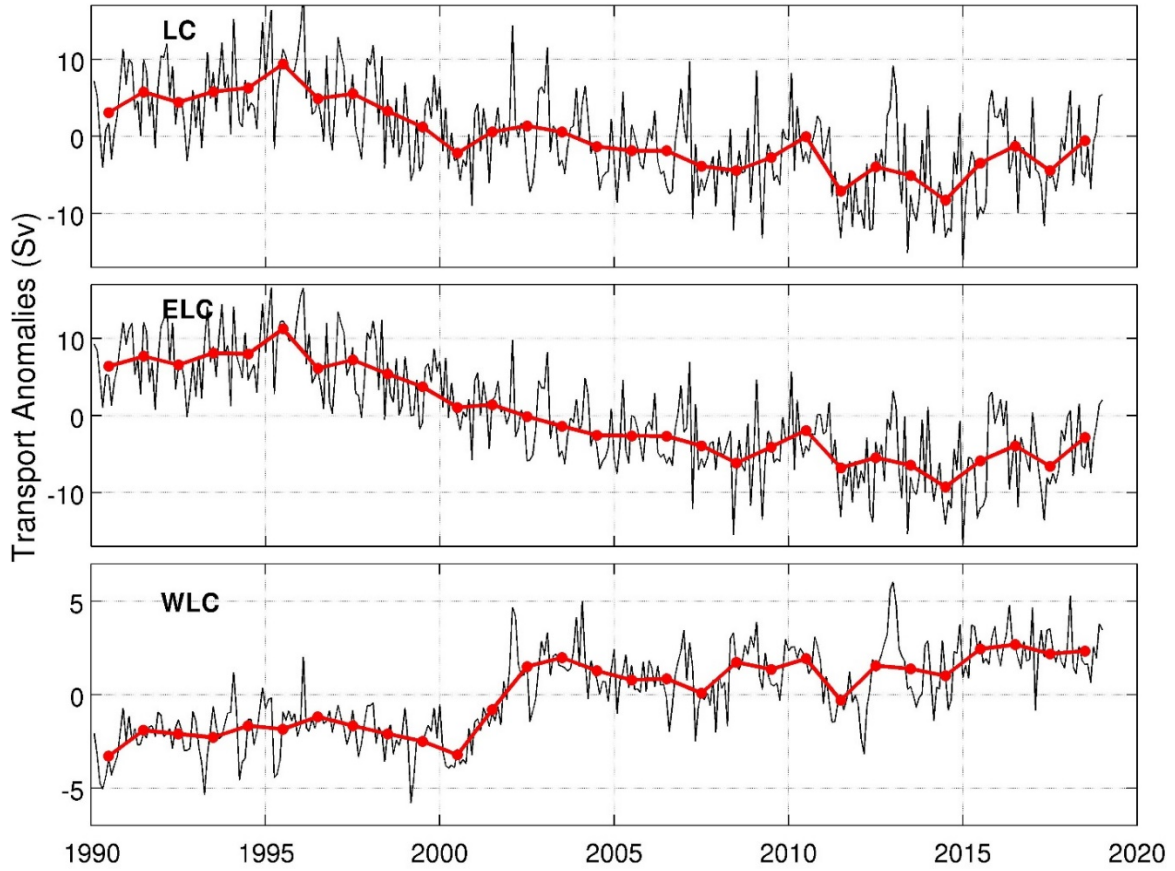
Figure 13. Transport anomalies of the LC, ELC, and WLC from 1990 to 2018.
Note: black lines are from the monthly data, and red lines and dots are from the annual means.
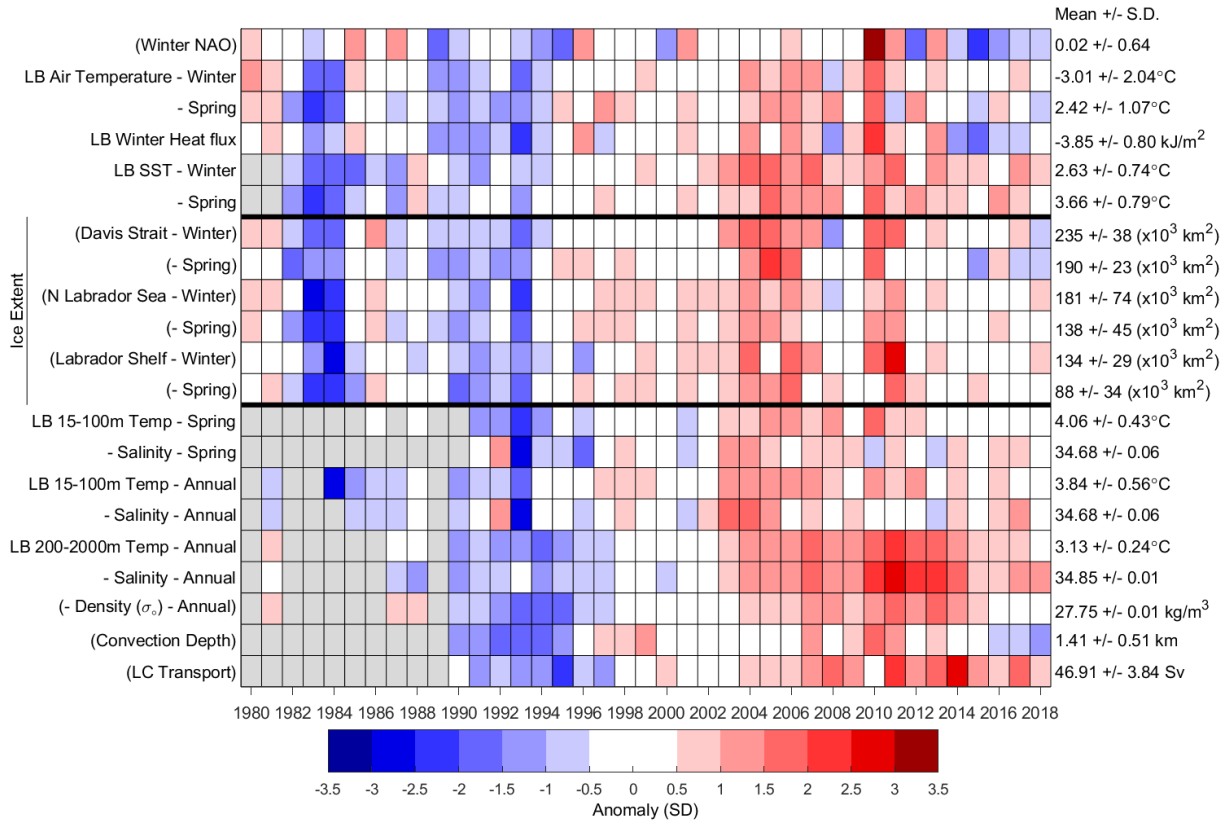
Figure 14. Scorecard for 1980–2018 oceanographic series. A grey cell indicates missing data, a white cell is a value within 0.5 SD of the long-term mean based on data from 1981–2010 when possible; a red cell indicates above normal conditions, and a blue cell below normal. Variables whose names appear in parentheses have reversed colour coding, whereby reds are lower than normal values that correspond to warm conditions. More intense colours indicate larger anomalies. Long-term means and standard deviations are shown on the right-hand side of the figure. North Atlantic Oscillation [NAO], Labrador Basin [LB], Labrador Current [LC].